

# Determination of $|V_{ub}|$ from Measurements of the Inclusive Charmless Semileptonic Partial Rates of $B$ Mesons using Full Reconstruction Tags

I. Bizjak,<sup>12</sup> K. Abe,<sup>7</sup> K. Abe,<sup>41</sup> H. Aihara,<sup>43</sup> Y. Asano,<sup>47</sup> S. Bahinipati,<sup>4</sup> A. M. Bakich,<sup>38</sup> Y. Ban,<sup>32</sup> E. Barberio,<sup>19</sup> M. Barbero,<sup>6</sup> A. Bay,<sup>16</sup> U. Bitenc,<sup>12</sup> S. Blyth,<sup>24</sup> A. Bondar,<sup>1</sup> A. Bozek,<sup>25</sup> M. Bračko,<sup>7, 18, 12</sup> J. Brodzicka,<sup>25</sup> T. E. Browder,<sup>6</sup> Y. Chao,<sup>24</sup> A. Chen,<sup>22</sup> W. T. Chen,<sup>22</sup> B. G. Cheon,<sup>3</sup> R. Chistov,<sup>11</sup> S.-K. Choi,<sup>5</sup> Y. Choi,<sup>37</sup> Y. K. Choi,<sup>37</sup> A. Chuvikov,<sup>33</sup> S. Cole,<sup>38</sup> J. Dalseno,<sup>19</sup> M. Danilov,<sup>11</sup> M. Dash,<sup>48</sup> L. Y. Dong,<sup>9</sup> A. Drutskoy,<sup>4</sup> S. Eidelman,<sup>1</sup> Y. Enari,<sup>20</sup> F. Fang,<sup>6</sup> S. Fratina,<sup>12</sup> N. Gabyshev,<sup>1</sup> A. Garmash,<sup>33</sup> T. Gershon,<sup>7</sup> G. Gokhroo,<sup>39</sup> B. Golob,<sup>17, 12</sup> A. Gorišek,<sup>12</sup> J. Haba,<sup>7</sup> T. Hara,<sup>30</sup> H. Hayashii,<sup>21</sup> M. Hazumi,<sup>7</sup> L. Hinz,<sup>16</sup> T. Hokuue,<sup>20</sup> Y. Hoshi,<sup>41</sup> S. Hou,<sup>22</sup> W.-S. Hou,<sup>24</sup> T. Iijima,<sup>20</sup> A. Imoto,<sup>21</sup> K. Inami,<sup>20</sup> A. Ishikawa,<sup>7</sup> R. Itoh,<sup>7</sup> M. Iwasaki,<sup>43</sup> Y. Iwasaki,<sup>7</sup> J. H. Kang,<sup>49</sup> J. S. Kang,<sup>14</sup> P. Kapusta,<sup>25</sup> N. Katayama,<sup>7</sup> H. Kawai,<sup>2</sup> T. Kawasaki,<sup>27</sup> H. R. Khan,<sup>44</sup> H. Kichimi,<sup>7</sup> H. J. Kim,<sup>15</sup> S. M. Kim,<sup>37</sup> K. Kinoshita,<sup>4</sup> S. Korpar,<sup>18, 12</sup> P. Križan,<sup>17, 12</sup> P. Krokovny,<sup>1</sup> R. Kulasiri,<sup>4</sup> S. Kumar,<sup>31</sup> C. C. Kuo,<sup>22</sup> A. Kuzmin,<sup>1</sup> Y.-J. Kwon,<sup>49</sup> G. Leder,<sup>10</sup> S. E. Lee,<sup>36</sup> T. Lesiak,<sup>25</sup> J. Li,<sup>35</sup> A. Limosani,<sup>7</sup> S.-W. Lin,<sup>24</sup> D. Liventsev,<sup>11</sup> J. MacNaughton,<sup>10</sup> G. Majumder,<sup>39</sup> F. Mandl,<sup>10</sup> T. Matsumoto,<sup>45</sup> A. Matyja,<sup>25</sup> Y. Mikami,<sup>42</sup> W. Mitaroff,<sup>10</sup> K. Miyabayashi,<sup>21</sup> H. Miyake,<sup>30</sup> H. Miyata,<sup>27</sup> R. Mizuk,<sup>11</sup> T. Nagamine,<sup>42</sup> Y. Nagasaka,<sup>8</sup> I. Nakamura,<sup>7</sup> E. Nakano,<sup>29</sup> M. Nakao,<sup>7</sup> Z. Natkaniec,<sup>25</sup> S. Nishida,<sup>7</sup> O. Nitoh,<sup>46</sup> T. Nozaki,<sup>7</sup> S. Ogawa,<sup>40</sup> T. Ohshima,<sup>20</sup> T. Okabe,<sup>20</sup> S. Okuno,<sup>13</sup> S. L. Olsen,<sup>6</sup> Y. Onuki,<sup>27</sup> W. Ostrowicz,<sup>25</sup> P. Pakhlov,<sup>11</sup> H. Park,<sup>15</sup> N. Parslow,<sup>38</sup> L. S. Peak,<sup>38</sup> R. Pestotnik,<sup>12</sup> L. E. Piilonen,<sup>48</sup> M. Rozanska,<sup>25</sup> H. Sagawa,<sup>7</sup> Y. Sakai,<sup>7</sup> N. Sato,<sup>20</sup> T. Schietinger,<sup>16</sup> O. Schneider,<sup>16</sup> P. Schönmeier,<sup>42</sup> C. Schwanda,<sup>10</sup> K. Senyo,<sup>20</sup> M. E. Sevier,<sup>19</sup> H. Shibuya,<sup>40</sup> B. Shwartz,<sup>1</sup> V. Sidorov,<sup>1</sup> A. Somov,<sup>4</sup> N. Soni,<sup>31</sup> R. Stamen,<sup>7</sup> S. Stanič,<sup>28</sup> M. Starič,<sup>12</sup> T. Sumiyoshi,<sup>45</sup> S. Suzuki,<sup>34</sup> S. Y. Suzuki,<sup>7</sup> O. Tajima,<sup>7</sup> F. Takasaki,<sup>7</sup> K. Tamai,<sup>7</sup> N. Tamura,<sup>27</sup> M. Tanaka,<sup>7</sup> Y. Teramoto,<sup>29</sup> X. C. Tian,<sup>32</sup> T. Tsuboyama,<sup>7</sup> T. Tsukamoto,<sup>7</sup> S. Uehara,<sup>7</sup> T. Uglov,<sup>11</sup> K. Ueno,<sup>24</sup> S. Uno,<sup>7</sup> P. Urquijo,<sup>19</sup> G. Varner,<sup>6</sup> K. E. Varvell,<sup>38</sup> S. Villa,<sup>16</sup> C. C. Wang,<sup>24</sup> C. H. Wang,<sup>23</sup> Y. Watanabe,<sup>44</sup> Q. L. Xie,<sup>9</sup> B. D. Yabsley,<sup>48</sup> A. Yamaguchi,<sup>42</sup> Y. Yamashita,<sup>26</sup> M. Yamauchi,<sup>7</sup> Heyoung Yang,<sup>36</sup> L. M. Zhang,<sup>35</sup> Z. P. Zhang,<sup>35</sup> V. Zhilich,<sup>1</sup> and D. Žontar<sup>17, 12</sup>

(The Belle Collaboration)

<sup>1</sup>*Budker Institute of Nuclear Physics, Novosibirsk*

<sup>2</sup>*Chiba University, Chiba*

<sup>3</sup>*Chonnam National University, Kwangju*

<sup>4</sup>*University of Cincinnati, Cincinnati, Ohio 45221*

<sup>5</sup>*Gyeongsang National University, Chinju*

<sup>6</sup>*University of Hawaii, Honolulu, Hawaii 96822*

<sup>7</sup>*High Energy Accelerator Research Organization (KEK), Tsukuba*

<sup>8</sup>*Hiroshima Institute of Technology, Hiroshima*

<sup>9</sup>*Institute of High Energy Physics, Chinese Academy of Sciences, Beijing*

<sup>10</sup>*Institute of High Energy Physics, Vienna*

<sup>11</sup>*Institute for Theoretical and Experimental Physics, Moscow*

<sup>12</sup>*J. Stefan Institute, Ljubljana*

<sup>13</sup>*Kanagawa University, Yokohama*

<sup>14</sup>*Korea University, Seoul*

<sup>15</sup>*Kyungpook National University, Taegu*

<sup>16</sup>*Swiss Federal Institute of Technology of Lausanne, EPFL, Lausanne*

<sup>17</sup>*University of Ljubljana, Ljubljana*

<sup>18</sup>*University of Maribor, Maribor*

<sup>19</sup>*University of Melbourne, Victoria*

<sup>20</sup>*Nagoya University, Nagoya*

<sup>21</sup>*Nara Women's University, Nara*

<sup>22</sup>*National Central University, Chung-li*

<sup>23</sup>*National United University, Miao Li*

<sup>24</sup>*Department of Physics, National Taiwan University, Taipei*

<sup>25</sup>*H. Niewodniczanski Institute of Nuclear Physics, Krakow*

<sup>26</sup>*Nippon Dental University, Niigata*

<sup>27</sup>*Niigata University, Niigata*

<sup>28</sup>*Nova Gorica Polytechnic, Nova Gorica*

<sup>29</sup>*Osaka City University, Osaka*

<sup>30</sup>*Osaka University, Osaka*

<sup>31</sup>*Panjab University, Chandigarh*

- <sup>32</sup>*Peking University, Beijing*  
<sup>33</sup>*Princeton University, Princeton, New Jersey 08544*  
<sup>34</sup>*Saga University, Saga*  
<sup>35</sup>*University of Science and Technology of China, Hefei*  
<sup>36</sup>*Seoul National University, Seoul*  
<sup>37</sup>*Sungkyunkwan University, Suwon*  
<sup>38</sup>*University of Sydney, Sydney NSW*  
<sup>39</sup>*Tata Institute of Fundamental Research, Bombay*  
<sup>40</sup>*Toho University, Funabashi*  
<sup>41</sup>*Tohoku Gakuin University, Tagajo*  
<sup>42</sup>*Tohoku University, Sendai*  
<sup>43</sup>*Department of Physics, University of Tokyo, Tokyo*  
<sup>44</sup>*Tokyo Institute of Technology, Tokyo*  
<sup>45</sup>*Tokyo Metropolitan University, Tokyo*  
<sup>46</sup>*Tokyo University of Agriculture and Technology, Tokyo*  
<sup>47</sup>*University of Tsukuba, Tsukuba*  
<sup>48</sup>*Virginia Polytechnic Institute and State University, Blacksburg, Virginia 24061*  
<sup>49</sup>*Yonsei University, Seoul*

We present a measurement of the Cabibbo-Kobayashi-Maskawa matrix element  $|V_{ub}|$ , based on  $253 \text{ fb}^{-1}$  of data collected by the Belle detector at the KEKB  $e^+e^-$  asymmetric collider. Events are tagged by fully reconstructing one of the  $B$  mesons, produced in pairs from  $\Upsilon(4S)$ . The signal for  $b \rightarrow u$  semileptonic decay is distinguished from the  $b \rightarrow c$  background using the hadronic mass  $M_X$ , the leptonic invariant mass squared  $q^2$  and the variable  $P_+ \equiv E_X - |\vec{p}_X|$ . The results are obtained for events with the prompt-lepton momentum,  $p_\ell^* \geq 1 \text{ GeV}/c$ , in three kinematic regions (1)  $M_X < 1.7 \text{ GeV}/c^2$ , (2)  $M_X < 1.7 \text{ GeV}/c^2$  combined with  $q^2 > 8 \text{ GeV}^2/c^2$ , and by (3)  $P_+ < 0.66 \text{ GeV}/c$ , allowing for a comparison of the three methods. The matrix element  $|V_{ub}|$  is found to be  $(4.09 \pm 0.19 \pm 0.20^{+0.14}_{-0.15} \pm 0.18) \times 10^{-3}$ , where the errors are statistical, systematic including Monte Carlo modeling, theoretical and from shape function parameter determination, respectively.

PACS numbers: 12.15.Hh, 11.30.Er, 13.25.Hw

An accurate knowledge of the Cabibbo-Kobayashi-Maskawa matrix element  $|V_{ub}|$  is crucial to test Standard Model predictions for  $CP$  violation. Currently, the best precision may be achieved by measuring the inclusive rate  $\Delta\Gamma_{u\ell\nu}(\Delta\Phi)$  of  $B \rightarrow X_u\ell\nu$  decays in a restricted region of the phase space ( $\Delta\Phi$ ) where the dominant charm background is suppressed and theoretical uncertainties are minimized. The theoretical factor  $R(\Delta\Phi)$  directly relates the inclusive rate to  $|V_{ub}|$ , with no extrapolation to the full phase space:  $|V_{ub}|^2 = \Delta\Gamma_{u\ell\nu}(\Delta\Phi)/R(\Delta\Phi)$ . Here we report measurements of  $\Delta\Gamma_{u\ell\nu}(\Delta\Phi)$  for several choices of  $\Delta\Phi$  and derive the corresponding values of  $|V_{ub}|$ .

The measurements are made with a sample of events where the hadronic decay mode of the tagging side  $B$  meson,  $B_{\text{tag}}$ , is fully reconstructed, while the semileptonic decay of the signal side  $B$  meson,  $B_{\text{sig}}$ , is identified by the presence of a high momentum electron or muon.  $B$  denotes both charged and neutral  $B$  mesons. This method allows the construction of the invariant masses of the hadronic ( $M_X$ ) and leptonic ( $\sqrt{q^2}$ ) system in the semileptonic decay, and the variable  $P_+ \equiv E_X - |\vec{p}_X|$ , where  $E_X$  is the energy and  $|\vec{p}_X|$  the magnitude of the three-momentum of the hadronic system. These inclusive kinematic variables can be used to separate the  $B \rightarrow X_u\ell\nu$  decays from the much more abundant  $B \rightarrow X_c\ell\nu$  decays. Three competing kinematic regions ( $\Delta\Phi$ ) were proposed

by theoretical studies [1, 2], based on the three kinematic variables, and are directly compared by this analysis. The value of  $|V_{ub}|$  is extracted using recent theoretical calculations [2, 3] that include all the currently known contributions.  $M_X$  and  $q^2$  selections were already used to extract  $|V_{ub}|$  [4, 5]. The present analysis is the first one to use  $P_+$  and to directly compare the three methods.

The data were collected with the Belle detector [6] at the asymmetric-energy KEKB storage ring [7]. The results presented in this paper are based on a  $253 \text{ fb}^{-1}$  sample recorded at the  $\Upsilon(4S)$  resonance, which contains  $275 \times 10^6 B\bar{B}$  pairs. An additional  $28 \text{ fb}^{-1}$  sample taken at a center-of-mass energy  $60 \text{ MeV}$  below the  $\Upsilon(4S)$  resonance is used to subtract the background from  $e^+e^- \rightarrow q\bar{q}$  ( $q = u, d, s, c$ ).

Monte Carlo (MC) simulated events were used to determine efficiencies as well as signal and background distributions. The detector simulation was based on GEANT [8]. To model  $B \rightarrow X_u\ell\nu$  we use the EvtGen generator [9] with various models, where  $X_u$  is  $\pi$  or  $\rho$  [10], an excited  $X_u$  state [11], or a non-resonant multiparticle final state [12]. The  $B \rightarrow X_c\ell\nu$  transitions are simulated according to the QQ generator [13]. For the two dominant contributions,  $D^*\ell\nu$  and  $D\ell\nu$ , we use an HQET-based parametrization of form factors [14] and ISGW2 model [11], respectively. For the  $D^{**}$  we use

ISGW2 model and for sub-components  $D_1$  and  $D_2^*$  set  $\frac{B \rightarrow D_1 \ell \nu + B \rightarrow D_2^* \ell \nu}{B \rightarrow D^{**} \ell \nu} = 0.35 \pm 0.23$ . The motion of the  $b$  quark inside the  $B$  meson is implemented with the introduction of a shape function [12, 15] that describes the  $b$  quark momentum distribution inside the  $B$  meson.

The  $B_{\text{tag}}$  candidates are reconstructed in the modes  $B \rightarrow D^{(*)} \pi / \rho / a_1 / D_s^{(*)}$ ,  $\bar{D}^0 \rightarrow K^+ \pi^-$ ,  $K^+ \pi^- \pi^0$ ,  $K^+ \pi^+ \pi^- \pi^-$ ,  $K_S^0 \pi^0$ ,  $K_S^0 \pi^+ \pi^-$ ,  $K_S^0 \pi^+ \pi^- \pi^0$  and  $K^+ K^-$ ,  $D^- \rightarrow K^+ \pi^- \pi^-$ ,  $K^+ \pi^- \pi^- \pi^0$ ,  $K_S^0 \pi^-$ ,  $K_S^0 \pi^- \pi^0$ ,  $K_S^0 \pi^- \pi^- \pi^+$  and  $K^+ K^- \pi^-$ , and  $D_s^+ \rightarrow K_S^0 K^+$  and  $K^+ K^- \pi^+$ .  $\bar{D}^*$  mesons are reconstructed by combining a  $\bar{D}$  candidate and a soft pion or photon. (Inclusion of charge conjugate decays is implied throughout this paper.) The selection of  $B_{\text{tag}}$  candidates is based on the beam-constrained mass,  $M_{\text{bc}} = \sqrt{E_{\text{beam}}^{*2}/c^4 - p_B^{*2}/c^2}$ , and the energy difference,  $\Delta E = E_B^* - E_{\text{beam}}^*$ . Here  $E_{\text{beam}}^* = \sqrt{s}/2 \simeq 5.290 \text{ GeV}$  is the beam energy in the  $e^+e^-$  center-of-mass system (cms), and  $p_B^*$  and  $E_B^*$  are the cms momentum and energy of the reconstructed  $B$  meson. (Throughout this paper the variables calculated in the cms are denoted with an asterisk.)

The combinatorial background from jet-like  $e^+e^- \rightarrow q\bar{q}$  processes is suppressed by an event topology requirement based on the normalized second Fox-Wolfram moment  $R_2 < 0.5$  [16], and for some modes also by  $|\cos \theta_{\text{thrust}}^*| < 0.8$ , where  $\theta_{\text{thrust}}^*$  is the angle between the thrust axis of the  $B_{\text{tag}}$  candidate and that of the rest of the event. To minimize the fraction of events with incorrect separation of tag and signal sides while maintaining high signal efficiency, a loose selection requirement of  $M_{\text{bc}} \geq 5.22 \text{ GeV}/c^2$  and  $-0.2 < \Delta E < 0.05 \text{ GeV}$  is made. If an event has multiple  $B_{\text{tag}}$  candidates, we choose the one having the smallest  $\chi^2$  based on  $\Delta E$ , the  $D$  candidate mass, and the  $D^* - D$  mass difference if applicable.

For events tagged by fully reconstructed  $B_{\text{tag}}$  candidates, we search for electrons or muons from semileptonic decays of  $B_{\text{sig}}$ . We require a lepton with momentum  $p_\ell^*$  exceeding  $1 \text{ GeV}/c$  in the laboratory polar angular region of  $26^\circ \leq \theta \leq 140^\circ$ . Leptons from  $J/\psi$  decay, photon conversion in the material of the detector, and  $\pi^0$  decay are rejected based on the invariant mass they form in combination with an oppositely charged lepton and for electron candidates also with an additional photon. When the  $B_{\text{tag}}$  candidate is charged, we also require the lepton charge to be consistent with that from prompt semileptonic decay. The signal yield is obtained by fitting the  $M_{\text{bc}}$  distribution to the sum of an empirical parametrization of the combinatorial background shape [17] plus a signal shape [18] that peaks at the  $B$  mass and taking the part of the signal that lies in the “signal region,”  $M_{\text{bc}} \geq 5.27 \text{ GeV}/c^2$ , as shown in Fig. 1(a). The cut-off for  $M_{\text{bc}}$  reduces the uncertainty from the incorrect assignment of tag and signal sides in signal events.

The  $B \rightarrow X_u \ell \nu$  signal events are selected by re-

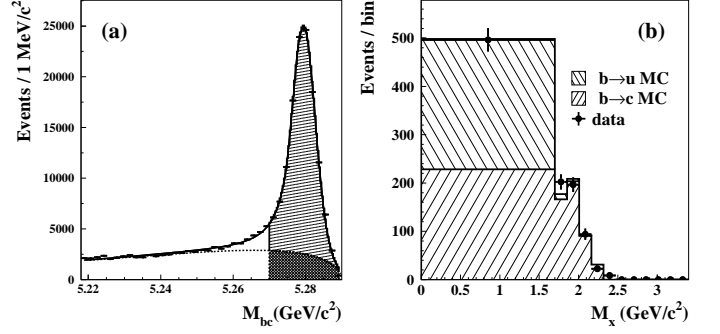


FIG. 1: (a) Distribution in  $M_{\text{bc}}$  (data) of  $B_{\text{tag}}$  candidates in events satisfying  $B_{\text{sig}}$  selection. (b)  $M_X$  distribution for events with  $q^2 > 8 \text{ GeV}^2/c^2$ , with fitted contributions of  $B \rightarrow X_c \ell \nu$  and  $B \rightarrow X_u \ell \nu$ .

moving poorly measured soft charged tracks and imposing several additional requirements to reject poorly reconstructed events and suppress the  $B \rightarrow X_c \ell \nu$  background. We require that the event contain exactly one lepton and have zero net charge and that the invariant mass squared of the missing four-momentum  $m_{\text{miss}}^2 \equiv (p_{\Upsilon(4S)} - p_{B_{\text{tag}}} - p_X - p_\ell)^2$  ( $p_{\Upsilon(4S)}$ ,  $p_{B_{\text{tag}}}$  and  $p_X$  are four-momenta of the  $\Upsilon(4S)$ ,  $B_{\text{tag}}$ , and hadronic system ( $X$ ), respectively) be within  $-1 \leq m_{\text{miss}}^2 \leq 0.5 \text{ GeV}^2/c^4$ . To suppress the  $B \rightarrow X_c \ell \nu$  background, events with a  $K^\pm$  or  $K_S^0$  candidate on the signal side are rejected (kaon veto). To reject events containing a  $K_L^0$ , we require that the angle between the missing momentum and the direction of any  $K_L^0$  candidate, reconstructed in the  $K_L^0$  detector, be greater than 37 degrees. We also reject  $B^0 \rightarrow D^{*+} \ell^- \bar{\nu}$  events by detecting the slow pion ( $\pi_s$ ) from  $D^{*+} \rightarrow D^0 \pi_s^+$  and deducing from its momentum the momentum of the  $D^{*+}$ . The missing mass squared  $m_{\text{miss}}^2(D^*) = (p_B - p_{D^*} - p_\ell)^2$  is calculated from the reconstructed quantities, and events with  $m_{\text{miss}}^2(D^*) > -3 \text{ GeV}^2/c^4$  are rejected.

Finally, the kinematic variables  $M_X$  and  $P_+$  are calculated from the measured momenta of all charged tracks and energy deposits of all neutral clusters in the electromagnetic calorimeter that are not used in the  $B_{\text{tag}}$  reconstruction or for the lepton candidate. The four-momentum of the leptonic system is calculated as  $q = p_{\Upsilon(4S)} - p_{B_{\text{tag}}} - p_X$ . The distributions of events in  $M_X$  and  $P_+$  are obtained by fitting the  $M_{\text{bc}}$  distribution, as described above, in bins of  $M_X$  and  $P_+$ . Figures 1(b), 2(a) and 3(a) show the resulting  $M_X$  and  $P_+$  distributions. We define three kinematic signal regions ( $\Delta\Phi$ ) for events where the prompt lepton has  $p_\ell^* \geq 1 \text{ GeV}/c$ :  $P_+ < 0.66 \text{ GeV}/c$ ,  $M_X < 1.7 \text{ GeV}/c^2$ , and  $M_X < 1.7 \text{ GeV}/c^2$  combined with  $q^2 > 8 \text{ GeV}^2/c^2$ . These three regions are denoted as  $P_+$ ,  $M_X$  and  $M_X/q^2$ , respectively. To minimize the systematic effects of uncertainties in lepton selection and full reconstruction, we normalize the partial rate for each signal region with the total semileptonic

TABLE I:  $N_{b \rightarrow u}^{\text{raw}}$ ,  $\varepsilon_{\text{sel}}^{b \rightarrow u}$ ,  $F$  and  $r_{b \rightarrow u}^{\text{sl}}$  for the three kinematic signal regions.

$\Delta\Phi$	$N_{b \rightarrow u}^{\text{raw}}$	$\varepsilon_{\text{sel}}^{b \rightarrow u}$	$F$	$r_{b \rightarrow u}^{\text{sl}}$
$M_X/q^2$	$268 \pm 27$	26.5%	1.03	$0.687 \pm 0.014$
$M_X$	$404 \pm 37$	28.7%	1.07	$0.700 \pm 0.011$
$P_+$	$340 \pm 32$	25.5%	1.01	$0.700 \pm 0.012$

rate:

$$W = \frac{\Delta\Gamma_{u\ell\nu}(\Delta\Phi)}{\Gamma(X\ell\nu)} = \frac{N_{b \rightarrow u}^{\text{raw}}}{N_{\text{sl}}} \times \frac{F}{\varepsilon_{\text{sel}}^{b \rightarrow u}} \times \frac{\varepsilon_{\text{frec}}^{\text{sl}}}{\varepsilon_{\text{frec}}^{b \rightarrow u}} \times \frac{\varepsilon_{\ell}^{\text{sl}}}{\varepsilon_{\ell}^{b \rightarrow u}}. \quad (1)$$

To extract the raw number of signal events,  $N_{b \rightarrow u}^{\text{raw}}$ , we fit the  $M_X$  and  $P_+$  distributions with MC-determined shapes for  $B \rightarrow X_u\ell\nu$  and  $B \rightarrow X_c\ell\nu$  and subtract the  $B \rightarrow X_c\ell\nu$  contribution. The results for the  $M_X/q^2$  and  $P_+$  regions are shown in Figs. 1(b) and 2(a), respectively. MC simulation is used to estimate the conversion factor  $F$  of the observed number of events  $N_{b \rightarrow u}^{\text{raw}}$  to the number of signal events produced in the region in question and observed anywhere, and to estimate the efficiency for these events,  $\varepsilon_{\text{sel}}^{b \rightarrow u}$ .

$N_{\text{sl}} = (9.14 \pm 0.05) \times 10^4$  is the number of events having at least one lepton with  $p_{\ell}^* \geq 1 \text{ GeV}/c$ , determined from a fit to the corresponding  $M_{bc}$  distribution (Fig. 1(a)), and corrected for the expected fraction of background events from non-semileptonic decays (14.0%), as estimated by MC simulation. The factor  $\varepsilon_{\text{frec}}^{\text{sl}}/\varepsilon_{\text{frec}}^{b \rightarrow u}$  accounts for a possible difference in the  $B_{\text{tag}}$  reconstruction efficiency in the presence of a semileptonic or  $B \rightarrow X_u\ell\nu$  decay;  $\varepsilon_{\ell}^{\text{sl}}/\varepsilon_{\ell}^{b \rightarrow u}$  is the ratio of both lepton identification efficiencies and fractions of semileptonic decay leptons with  $p_{\ell}^* \geq 1 \text{ GeV}/c$ , in the whole kinematic phase space for semileptonic decays, and within the kinematic signal region for signal events. The product of efficiency ratios  $r_{b \rightarrow u}^{\text{sl}} \equiv \varepsilon_{\text{frec}}^{\text{sl}}/\varepsilon_{\text{frec}}^{b \rightarrow u} \times \varepsilon_{\ell}^{\text{sl}}/\varepsilon_{\ell}^{b \rightarrow u}$  is obtained from MC simulation. Table I summarizes the results for  $N_{b \rightarrow u}^{\text{raw}}$ ,  $\varepsilon_{\text{sel}}^{b \rightarrow u}$ ,  $F$  and  $r_{b \rightarrow u}^{\text{sl}}$  for all three signal regions, where the error in  $N_{b \rightarrow u}^{\text{raw}}$  is statistical only. Inserting these values in Eq. 1, we obtain the three values of  $W$ . As both numerator and denominator of  $W$  have been obtained from the same tag sample, the  $B^0/B^+$  weightings are the same, and  $W$  has no dependence on lifetimes. Multiplying  $W$  by the average measured semileptonic rate  $\Gamma(X\ell\nu) = \mathcal{B}(B \rightarrow X\ell\nu)/\tau_B$ , obtained from  $\mathcal{B}(B \rightarrow X\ell\nu) = 0.1073 \pm 0.0028$  and  $\tau_B = (1.604 \pm 0.016) \text{ ps}$  [19], gives the average  $\Delta\Gamma_{u\ell\nu}(\Delta\Phi)$ . The results with relative errors are given in Table II.

We divide the experimental error into four categories: statistical, systematic,  $b \rightarrow c$  and  $b \rightarrow u$  MC modeling errors, and summarize them in Table II for the three  $\Delta\Gamma_{u\ell\nu}(\Delta\Phi)$  measurements. The two modeling errors include the uncertainty in signal event extraction, efficiency and unfolding factor determination due to the

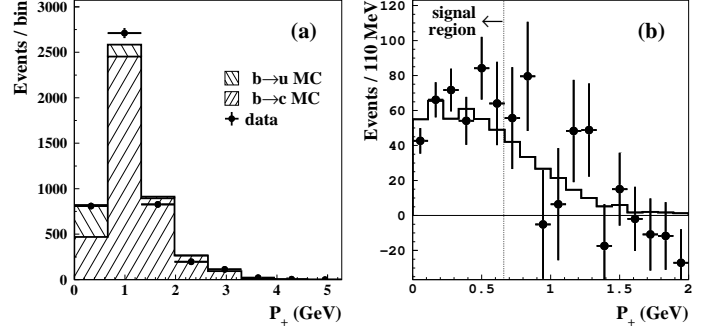


FIG. 2: (a) The  $P_+$  distribution for the selected events, with fitted contributions from  $B \rightarrow X_c\ell\nu$  and  $B \rightarrow X_u\ell\nu$ , (b)  $P_+$  distribution (symbols with error bars) after subtracting  $B \rightarrow X_c\ell\nu$ , with fitted  $B \rightarrow X_u\ell\nu$  contribution (histogram).

TABLE II: Partial rates to the three kinematic signal regions with relative errors (in %).

$\Delta\Phi$	$\Delta\Gamma_{u\ell\nu}(\Delta\Phi)$	stat	syst	$b \rightarrow u$	$b \rightarrow c$
$M_X/q^2$	$5.24 \times 10^{-4} \text{ ps}^{-1}$	10.0	8.9	6.2	5.3
$M_X$	$7.71 \times 10^{-4} \text{ ps}^{-1}$	9.1	7.1	6.1	2.2
$P_+$	$6.89 \times 10^{-4} \text{ ps}^{-1}$	9.4	9.3	6.4	8.7

choice of specific theoretical models and values of the parameters used in our MC predictions. For signal  $B \rightarrow X_u\ell\nu$  MC, the shape function parameters  $\Lambda^{\text{SF}} = (0.66 \pm 0.15) \text{ GeV}/c^2$  and  $\lambda_1^{\text{SF}} = -(0.40 \pm 0.20) \text{ GeV}^2/c^2$  were varied within the stated limits, taking into account the negative correlation between them [20]. To take into account the uncertainty of the prediction in Ref. [12], we use a factor of two larger error for  $\Lambda^{\text{SF}}$  than was determined in Ref. [20]. For  $B \rightarrow X_c\ell\nu$  MC, the uncertainty due to our limited knowledge of branching fractions is studied by varying the contributions of  $D\ell\nu$  and  $D^*\ell\nu$  and the relative fraction of narrow states  $D_1$  and  $D_2^*$  that contribute to  $D^{**}\ell\nu$  to estimate the modeling error of the

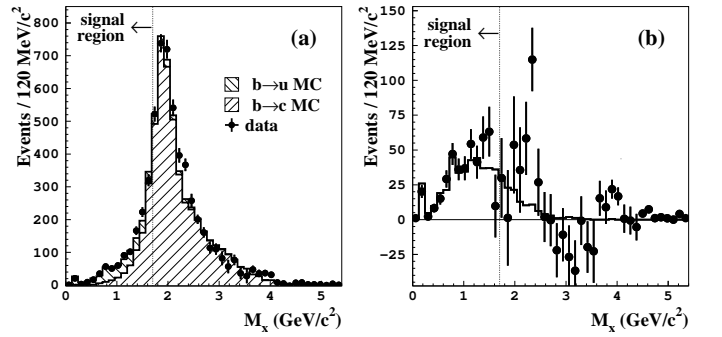


FIG. 3:  $M_X$  distribution (no  $q^2$  requirement) with fitted contributions from  $X_c\ell\nu$  and  $X_u\ell\nu$ : (a) before and (b) after subtracting the  $X_c\ell\nu$  contribution (symbols with error bars), shown with the prediction for  $X_u\ell\nu$  (MC, histogram).



$D^{**}$  region. The uncertainty from form factor modeling in  $D\ell\nu$  and  $D^*\ell\nu$  was studied by varying the parameters  $\rho_D^2 = 1.15 \pm 0.16$  and  $\rho_A^2 = 1.56 \pm 0.13$  within their errors [19]. The validity of the  $B \rightarrow X_c \ell \nu$  simulation was tested on a  $B \rightarrow X_c \ell \nu$  enhanced control sample, where all selection requirements are applied but with the kaon veto reversed. The kinematic distributions of this control sample are accurately described by the simulation. Other sources of uncertainties, namely limited MC statistics, extraction of  $r_{b \rightarrow u}^{\text{sl}}$ , fitting procedure and imperfect detector simulation are combined in the systematic error. The uncertainties due to inaccurate simulation of tracking, particle identification, and cluster finding are estimated by varying for each source the efficiency within the expected error and taking the maximum change in  $\Delta\Gamma_{ul\nu}(\Delta\Phi)$  as the error. For each of these sources the effects on simulated  $b \rightarrow u$  and  $b \rightarrow c$  events are correlated, and the associated shifts are summed linearly. The net contributions from the three sources are then summed in quadrature.

The CKM matrix element  $|V_{ub}|$  is obtained directly from the partial rate using  $|V_{ub}|^2 = \Delta\Gamma_{ul\nu}(\Delta\Phi)/R(\Delta\Phi)$ .  $R(\Delta\Phi)$  is the theoretical prediction of  $\Delta\Gamma_{ul\nu}(\Delta\Phi)$ , the partial rate with a prompt lepton with  $p_\ell^* \geq 1 \text{ GeV}/c$ , divided by  $|V_{ub}|^2$ . The values of  $R$  (in  $\text{ps}^{-1}$ ) are calculated to be  $23.7 \pm 2.0(\text{SF})_{-2.3}^{+2.5}(\text{th.})$ ,  $46.1 \pm 4.2(\text{SF})_{-3.2}^{+3.5}(\text{th.})$  and  $39.4 \pm 4.5(\text{SF})_{-2.7}^{+2.8}(\text{th.})$  for the  $M_X/q^2$ ,  $M_X$  and  $P_+$  signal regions, respectively. The  $R(\Delta\Phi)$  values and their errors (SF) are calculated using the shape function scheme [15] parameters  $m_b(\text{SF}) = (4.60 \pm 0.04) \text{ GeV}/c^2$  and  $\mu_\pi^2(\text{SF}) = (0.20 \pm 0.04) \text{ GeV}^2/c^2$  with correlation coefficient  $\rho = -0.26$ , obtained from the result of a global fit to moments of both  $b \rightarrow c\ell\nu$  and  $b \rightarrow s\gamma$  distributions [21]. While the dependence of  $R(\Delta\Phi)$  on  $\mu_\pi^2(\text{SF})$  is small, we can approximate the dependence on  $m_b(\text{SF})$  as  $R/R(m_b^0) - 1 = k(\Delta\Phi) \cdot (m_b/m_b^0 - 1)$ , where  $m_b^0 = 4.60 \text{ GeV}/c^2$  and  $k(\Delta\Phi)$  is found to be 2.09, 2.29 and 3.00 for the  $M_X/q^2$ ,  $M_X$  and  $P_+$  signal regions, respectively. The theoretical error of  $R$  (th.) is estimated by varying the subleading shape functions (four models), the matching scales  $\mu_h$ ,  $\mu_i$ ,  $\bar{\mu}$  and weak annihilation [15]. The values of  $|V_{ub}|$  with errors are given in Table III. The total error on  $|V_{ub}|$  is 10%, 9% and 11% for  $M_X/q^2$ ,  $M_X$  and  $P_+$  regions, respectively. When the shape function parameters and  $R$  are better determined,  $|V_{ub}|$  can be recalculated from  $\Delta\Gamma_{ul\nu}(\Delta\Phi)$  shown in Table II.

The precision of the  $|V_{ub}|$  determination is better than previous measurements [4, 5, 22], owing to the use of larger data sample, better shape function parameter determination and improved theoretical predictions [2, 3]. We find that the usage of the variable  $P_+$  is more sensitive to  $b \rightarrow c$  modeling and shape function parametrization than the other two methods and will become competitive in the future when the theoretical error of  $R$  dominates. No significant experimental nor theoretical improvement was observed by applying the additional

TABLE III: Values for  $|V_{ub}|$  with relative errors (in %) for the three kinematic signal regions. Shape function parameters used in the calculation are  $m_b(\text{SF}) = (4.60 \pm 0.04) \text{ GeV}/c^2$  and  $\mu_\pi^2(\text{SF}) = (0.20 \pm 0.04) \text{ GeV}^2/c^2$ .

$\Delta\Phi$	$ V_{ub}  \times 10^3$	stat	syst	$b \rightarrow u$	$b \rightarrow c$	SF	th.
$M_X/q^2$	4.70	5.0	4.4	3.1	2.7	4.2	$_{-5.2}^{+4.8}$
$M_X$	4.09	4.6	3.5	3.1	1.1	4.5	$_{-3.8}^{+3.5}$
$P_+$	4.19	4.7	4.6	3.2	4.4	5.8	$_{-3.5}^{+3.4}$

selection  $q^2 > 8 \text{ GeV}^2/c^2$  to the  $M_X$  analysis. Taking correlations into account, we find that the difference between  $|V_{ub}|$  values for  $M_X/q^2$  and  $M_X$  regions has a significance of  $2.7\sigma$ . We conclude that the results are consistent within errors, but we do not rule out possible effects of duality violation or weak annihilation contribution. We chose the  $M_X$  signal region result for our  $|V_{ub}|$  determination, since it includes the largest portion of phase space and is least affected by the uncertainties:  $|V_{ub}| = (4.09 \pm 0.19 \pm 0.20_{-0.15}^{+0.14} \pm 0.18) \times 10^{-3}$ , where the errors are statistical, systematic with MC modeling, theoretical and from shape function parameter determination, respectively. The effectiveness of  $|V_{ub}|$  measurements using full reconstruction tagging is clear (Figs. 2(b) and 3(b)).

We thank the KEKB group for excellent accelerator operations, the KEK cryogenics group for efficient operation of the solenoid, and the KEK computer group and NII for valuable computing and Super-SINET network support. We acknowledge support from MEXT and JSPS (Japan); ARC and DEST (Australia); NSFC (contract No. 10175071, China); DST (India); the BK21 program of MOEHRD and the CHEP SRC program of KOSEF (Korea); KBN (contract No. 2P03B 01324, Poland); MIST (Russia); MHEST (Slovenia); SNSF (Switzerland); NSC and MOE (Taiwan); and DOE (USA).

We are grateful to B. Lange, M. Neubert and G. Paz for providing us with their theoretical computations implemented in an inclusive generator. We would specially like to thank M. Neubert for valuable discussions and suggestions.

- 
- [1] C. W. Bauer, Z. Ligeti and M. Luke, Phys. Rev. **D 64**, 113004 (2001).
  - [2] S. W. Bosch, B. O. Lange, M. Neubert and G. Paz, Phys Rev Lett. **93**, 221801(2004); Nucl. Phys. B **699**, 335 (2004).
  - [3] M. Neubert, Eur. Phys. J. C **40**, 165 (2005); Phys. Lett. B **612**, 13 (2005); hep-ph/0411027; S. W. Bosch, M. Neubert and G. Paz, JHEP **0411**, 073 (2004).
  - [4] B. Aubert *et al.* (BaBar Collaboration), Phys. Rev. Lett. **92**, 071802 (2004).

- [5] H. Kakuno *et al.* (Belle Collaboration), Phys. Rev. Lett. **92**, 101801 (2004).
- [6] A. Abashian *et al.* (Belle Collaboration), Nucl. Instrum. and Meth. A **479**, 117 (2002).
- [7] S. Kurokawa and E. Kikutani, Nucl. Instrum. and Meth. A **499**, 1 (2003), and other papers in this Volume.
- [8] R. Brun, F. Bruyant, M. Maire, A. C. McPherson and P. Zancarini, CERN Report No. DD/EE/84-1 (1984).
- [9] D. J. Lange, Nucl. Instrum. Meth. A **462**, 152(2001).
- [10] P. Ball, arXiv:hep-ph/0306251.
- [11] D. Scora and N. Isgur, Phys. Rev. D **52**, 2783 (1995).
- [12] F. De Fazio and M. Neubert, JHEP **9906**, 017 (1999).
- [13] QQ event generator, developed by CLEO Collaboration, see <http://www.lns.cornell.edu/public/CLEO/soft/qq>.
- [14] M. Neubert, Phys. Rept. **245**, 259 (1994).
- [15] B. O. Lange, M. Neubert and G. Paz, hep-ph/0504071 and private communication with M. Neubert.
- [16] G. C. Fox and S. Wolfram, Phys. Rev. Lett. **41**, 1581 (1978).
- [17] H. Albrecht *et al.* (ARGUS Collaboration), Z. Phys. C **48**, 543 (1990).
- [18] J. E. Gaiser *et al.*, Phys. Rev. D **34**, 711 (1986).
- [19] S. Eidelman *et al.*, Phys. Lett. B **592**, 1 (2004).
- [20] A. Limosani and T. Nozaki (Heavy Flavor Averaging Group), hep-ex/0407052.
- [21] O. Buchmueller and H. Flaecher (Heavy Flavor Averaging Group), hep-ph/0507253.
- [22] R. Barate *et al.* (ALEPH Collaboration), Eur. Phys. J. C **6**, 555 (1999); M. Acciarri *et al.* (L3 Collaboration), Phys. Lett. B **436** 174 (1998); P. Abreu *et al.* (DELPHI Collaboration), Phys. Lett. B **478** 14 (2000); G. Abbiendi *et al.* (OPAL Collaboration), Eur. Phys. J. C **21**, 399 (2001); A. Bornheim *et al.* (CLEO Collaboration), Phys. Rev. Lett. **88**, 231803 (2002)